

# Earthquake Response Analysis of Underground Tubular Structure

By Kenzo TOKI and Shiro TAKADA

(Manuscript received July 10, 1974)

## Abstract

The present paper deals with the vibrational characteristics of the longitudinal and transversal vibration of underground tubular structures subjected to earthquakes. The analytical model is composed of a cylindrical tubular structure of which axis is parallel to the ground surface and the surrounding ground is treated as an infinite homogeneous half space. From the analyses on the structural response to sinusoidal excitation, it was found that the vibration of the structure due to the inertia force will be hardly induced in the ground and that the dynamic motion of structure is strongly dominated by the ground motion. Moreover analyses on the axial and bending strains revealed that the axial strain is proportional to the velocity amplitude of the surrounding ground, while the bending strain is proportional to the acceleration amplitude. The results suggest that the velocity amplitude in the ground is the most significant factor in the aseismic design of underground pipe systems and the acceleration amplitude is of importance for the structures with large diameter such as subway tunnels. Response analyses of strains to strong motion accelerograms have been also performed by making use of the Fourier transform method. The analyses made clear that the effect of structural stiffness on the induced strain level is not so remarkable and the reduction of strain in structure from the strain in surrounding ground is of the order of 10 to 20%. Then the strain in ground is considered to be the upper bound of strain in structures.

## 1. Introduction

Earthquake resistant design of structures such as gas pipes, water pipes, subway tunnels and so forth can be classified as the same kind of structures from the view point of the seismic response analysis because such structures are constructed beneath the ground surface and they constitute network systems. In the present paper, these structures are hereafter specified as the underground tubular structures. Since this kind of structures are usually surrounded by soils, an interaction system is made up of the structure and ground. Although the subsurface structures such as a caisson resting in an upright position also constitutes an interaction system, the specific length in a horizontal direction is small compared with the wave length of a seismic wave and it is, therefore, possible to assume that there is no phase difference between any two points on a horizontal plane. On the other hand, in the underground tubular structure above defined, the long axis is essentially parallel to the ground surface and then there would be readily found any two arbitrary points which move out of phase of each other. Therefore the formulation of the problem should be performed from another point of view and it is necessary to establish a different approach of the analysis from the ordinary conception of the aseismic design which has been developed mainly for superstructures.

Various authors<sup>1)-6)</sup> have discussed the problem and vibrational characteristics of underground tubular structures. That which has been made clear to date may be summed up as follows; 1) The relative motion of underground tubular structure is very small compared with that of ground motion during earthquakes. 2) The natural vibration of such structures is hardly excited. 3) The amplitude of displacement of a structure does not exceed the amplitude of the surrounding ground. 4) Dynamic axial strains induced in any cross section of structures are generally greater than the bending strains of the structures with small diameter.

From the above summary it may be noticed that the distribution of the relative displacement along the structural axis and distribution of strain amplitude induced in ground are the most significant factors in the earthquake resistant design of underground tubular structures. Moreover it is readily recognized that the induced strain will be extensive when a seismic wave travels along the surface of the ground in which the local geology is complicated and varies from place to place.

In the present paper, theoretical analyses are performed employing the elastic wave transmission theory for a three dimensional model. Analytical models are composed of a cylindrical tubular structure of which long axis is parallel to the ground surface and the ground is treated as an infinite homogeneous elastic half space. Throughout the analysis it is assumed that the direction of the seismic wave transmission coincides with the structural axis. As for the wave velocity, the phase velocity of surface wave does not necessarily coincide to the velocity of body waves. Since the waves travelling along the ground surface are concerned in the present study, the different wave velocity from body wave velocities is assigned in the analyses.

## 2. Strain Amplitude to Sinusoidal Excitation

### 2.1 Axial Strain

As is shown in Fig. 1, the tubular structures are constructed under the ground surface and essentially parallel to the free surface of an elastic homogeneous space. In this figure  $a$  denotes the outer radius of structure and  $b$  is the inner radius. The cylindrical coordinates system  $(r, \theta, x)$  is set as shown in Fig. 1. Analysis is performed in a case that a tubular structure is subjected to a longitudinal seismic wave which travels along the structural axis. The incident wave at the ground far enough from

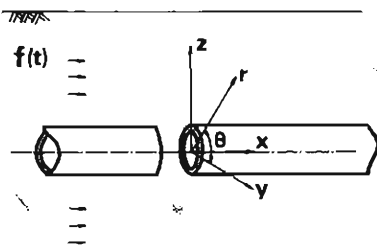


Fig. 1 Analytical model

the structure is expressed by

$$v^A = u_g^A \cdot \exp \{ik^A(x - c^A t)\} \tag{2.1}$$

where  $u_g^A$ ,  $k^A$  and  $c^A$  are the amplitude of displacement, the wave number and the phase velocity of the incident wave, respectively. Let  $u$  and  $w$  be the displacement in the direction of  $r$  and  $x$  coordinates respectively, then displacement components  $u$  and  $w$  are given by the following expressions considering the mode of the transmission of the incident wave.

$$u = U \cdot \exp \{ik^A(x - c^A t)\}, \quad w = W \cdot \exp \{ik^A(x - c^A t)\} \tag{2.2}$$

Substituting these expressions into the wave equations which govern the motion of the ground, the following results are obtained.

$$\left. \begin{aligned} u &= \left\{ A \frac{h^*}{h^2} H_1^{(1)}(h^*r) - B \frac{ik^A}{g^2} H_1^{(1)}(g^*r) \right\} \cdot \exp \cdot \{ik^A(x - c^A t)\} \\ w &= \left\{ -A \frac{ik^A}{h^2} H_0^{(1)}(h^*r) + B \frac{g^*}{g^2} H_0^{(1)}(g^*r) \right\} \cdot \exp \cdot \{ik^A(x - c^A t)\} \end{aligned} \right\} \tag{2.3}$$

where

$$\left. \begin{aligned} (h^*)^2 &= (w/v_l)^2 - (k^A)^2 = h^2 - (k^A)^2 \\ (g^*)^2 &= (w/v_r)^2 - (k^A)^2 = g^2 - (k^A)^2 \end{aligned} \right\} \tag{2.4}$$

and  $v_l$  and  $v_r$  are the dilatational and rotational wave velocities in the ground, respectively.  $H_n^{(1)}(z)$  is the Hankel function of the first kind and  $A$  and  $B$  are constants to be decided by boundary conditions.

As the effect of the transversal component of displacement is not so significant for the dynamic properties of the longitudinal direction of the system under consideration, in the present paper, therefore, radial displacement  $u$  is neglected. Then the longitudinal displacement  $w$  of the ground is calculated as follows;

$$w|_{r=a} \approx -A \frac{ik^A}{h^2} \left\{ H_0^{(1)}(h^*a) + \frac{g^*h^*}{(k^A)^2} \frac{H_1^{(1)}(h^*a)}{H_1^{(1)}(g^*a)} H_0^{(1)}(g^*a) \right\} \cdot \exp \{ik^A(x - c^A t)\} \tag{2.5}$$

From Eq. (2.5), surface traction  $\tau_{rx}$  which exerts on the contact plane of the structure with the surrounding ground is calculated as follows;

$$\tau_{rx}|_{r=a} = \mu \frac{\partial w}{\partial r} \Big|_{r=a} = i\mu A \left( \frac{g}{h} \right)^2 \frac{h^*}{k^A} H_1^{(1)}(h^*a) \tag{2.6}$$

Subsequently we deal with the axial vibration of the structure. At  $r=a$ , on the structural surface, the structure is in contact with the ground. Therefore the surrounding ground exerts a traction force on the structural surface, which is a function of the relative displacement of structure. Then the system under consideration is described as a kind of interaction system composed of the structure and ground. Denoting the amplitude of the structural deformation by  $u_d^A$ , the displacement of

structure  $u_p^A$  is written by

$$u_p^A = u_d^A \exp \{ik^A(x - c^A t)\} \quad (2.7)$$

Assuming no slip on the contact plane of structure with ground, the boundary condition is given by the following equation.

$$w|_{r=a} = u_p^A \quad (2.8)$$

Combining Eqs. (2.5), (2.7) and (2.8), constant  $A$  in Eq.(2.5) is solved in terms of  $u_d^A$  as follows;

$$A = -u_d^A / \left[ \frac{ik^A}{h^2} \left\{ H_0^{(1)}(h^*a) + \frac{g^*h^*}{k^2} \frac{H_0^{(1)}(g^*a)}{H_0^{(1)}(g^*a)} H_1^{(1)}(h^*a) \right\} \right] \quad (2.9)$$

On the other hand, the motion of the structure under the exertion of the restraint force  $F_x^A$  and inertia of ground is governed by the following differential equation

$$A_p \gamma \frac{\partial^2 u_p^A}{\partial t^2} - A_p E \frac{\partial^2 u_p^A}{\partial x^2} = -A_p \gamma \frac{\partial^2 v^A}{\partial t^2} - F_x^A \quad (2.10)$$

where,  $A_p$ ,  $\gamma$  and  $E$  are the cross sectional area, the volume density and Young's modulus of structure, respectively. And  $F_x^A$  is calculated from Eq.(2.6) as follows;

$$F_x^A = \int_0^{2\pi} a \tau_{rx} d\theta = \rho \pi a^2 \cdot \omega^2 \cdot f^A \cdot u_d^A \exp \{ik^A(x - c^A t)\} \quad (2.11)$$

where

$$\left. \begin{aligned} f^A &= -2 / \left[ F(h^*a) / \left\{ \left( \frac{c^A}{v_l} \right)^2 - 1 \right\} + F(g^*a) \right] \\ F(z) &= z H_0^{(1)}(z) / H_1^{(1)}(z) \end{aligned} \right\} \quad (2.12)$$

Concerning the restraint force given by Eq.(2.11),  $\rho \pi a^2$  is the mass of soil excluded by the structure and the magnitude of acceleration is  $\omega^2 u_d^A \cdot \exp \{ik^A(x - c^A t)\}$ . Then the quantity  $\rho \pi a^2 \omega^2 u_d^A \cdot \exp \{ik^A(x - c^A t)\}$  is referred to inertia force. If  $f^A$  in Eq.(2.12) were independent of frequency of an incident wave,  $f^A$  could be regarded as a coefficient of virtual mass. Frequency characteristics of  $f^A$  will be discussed in Section 5.

Substituting Eqs.(2.1) and (2.7) into Eq.(2.10), the absolute value of the displacement of the structure is obtained as follows;

$$U_p^A = \left\{ 1 + \frac{1}{\left( \frac{c^0}{c^A} \right)^2 - 1 + \frac{\rho}{\gamma} \frac{1}{1 - (b/a)^2} \cdot f^A} \right\} u_d^A \cdot \exp \{ik^A(x - c^A t)\} \quad (2.13)$$

where,  $(c^0 = E/\gamma)$  is the longitudinal wave velocity in the structure. From Eq.(2.13), normalized axial strain of the structure  $\varepsilon_A^*$  is determined by

$$\varepsilon_A^* \equiv \frac{\partial U_p^A}{\partial x} \cdot \frac{u_d^A}{a} = 2\pi \left( \frac{a}{\kappa^A} \right) \cdot i \cdot \frac{U_p^A}{u_d^A} \quad (2.14)$$

where  $\kappa^A$  is the wave length of the incident dilatational wave.  $f^A$  in Eq.(2.13) is a

complex function expressed in terms of the Hankel function with complex arguments. However under the following approximation, the definite value of  $f^A$  can be determined in terms of real variables. Namely, from Eq.(2.4),  $g^*a$  and  $h^*a$  are rewritten by the expressions

$$g^*a = 2\pi \frac{a}{\kappa^A} \sqrt{\left(\frac{c^A}{v_l}\right)^2 - 1}, \quad h^*a = 2\pi \frac{a}{\kappa^A} \sqrt{\left(\frac{c^A}{v_l}\right)^2 - 1} \quad (2.15)$$

Considering that the radius of structure is negligibly small compared with the wave length,  $\kappa^A$ ,  $g^*a$  and  $h^*a$  in Eq.(2.15) take very small values. When the argument of the Hankel function takes an imaginary value,  $f^A$  can be written by the modified Bessel function  $K_n(z)$  and the following relationship can be deduced.

$$f^A \approx 2/|\kappa|, \quad \kappa = g^*a \frac{K_0(g^*a)}{K_1(g^*a)} \quad (2.16)$$

For the set of values  $c^0/v_l=10.0$   $\nu=0.35$ ,  $b/a=0.95$   $c^A/v_l=1.5$  and  $K^A/a=100$ ,  $\{(c^0/c^A)^2-1\}$  in Eq.(2.13) takes the value of 43.3 and  $\rho f^A/\gamma\{1-(b/a)^2\}$  in Eq.(2.13) is 219.2. Therefore, it is reasonable to consider that the following inequality is valid generally.

$$\left| \left(\frac{c^0}{c^A}\right)^2 - 1 \right| < \left| \frac{\rho}{\gamma} \cdot \frac{1}{1-(b/a)^2} \cdot f^A \right|. \quad (2.17)$$

The left hand side term of the above inequality relates to the vibrational characteristics of the structure and the right hand side term is related to the restraining force acting on the structural surface. Furthermore, since the magnitude of the denominator of Eq.(2.13) is greater than that of the numerator, the following approximation is possible.

$$U_p^A \approx u_g^A \cdot \exp \{ik^A (x - c^A t)\} \quad (2.18)$$

According to Eq. (2.18), it follows that the displacement of the structure is close to that of the surrounding ground when the wave length of the seismic wave travelling along the axis of the structure is long enough compared with the radius of the structure. In other words, as far as the underground tubular structure such as pipes, tunnels and so on is concerned, vibrations of structures due to the inertia force of the structure will be hardly induced in the ground and the dynamic motions of structures are strongly dominated by the ground motions.

When the approximate result given by Eq. (2.18) is valid, the axial strain is readily calculated from Eq. (2.14) for the sinusoidal incident wave with amplitude  $u_g^A$  as follows.

$$\varepsilon_A^* \equiv \frac{\partial U_p^A}{\partial x} / \frac{u_g^A}{a} \approx 2\pi \left(\frac{a}{\kappa^A}\right) \quad (2.19)$$

And

$$\varepsilon_A \equiv \frac{\partial U_p^A}{\partial x} \approx u_g^A \left(\frac{2\pi}{\kappa^A}\right) \quad (2.20)$$

Considering that  $2\pi/\kappa^A = \omega/c^A$  and that  $\omega u_0^A$  is replaced by velocity amplitude, Eq. (2.20) implies that the axial strain in a tubular structure is proportional to the velocity amplitude of surrounding ground under the assumption that the displacement of structure is approximated by that of the ground. These results are significant and comprehensive for the earthquake resistant design of this kind of structures under consideration and permit us to infer the strain or stress in structures if we could estimate the velocity amplitude of the ground during earthquakes. As velocity records can be computed from accelerograms by numerical integration, this procedure is usually possible and not so troublesome.

## 2.2 Bending Strain

Flexural vibration of a underground tubular structure is analysed for the case that the structure is subjected to a *SH* wave travelling along the axis of the structure with velocity  $c^B$ . The similar analytical model with that used in the previous analyses is set up. An incident seismic wave in the ground far enough from the structure is written as follows.

$$v^B = u_0^B \exp \{ik^B (x - c^B t)\} \quad (2.21)$$

where  $u_0^B$ ,  $k^B$  and  $c^B$  are the displacement amplitude, the wave length and the phase velocity of the incident wave, respectively. After the manner of the analysis for the longitudinal vibration, relative displacements  $u$  and  $v$  in ground are calculated by solving the wave equations governing the transversal motion of an infinite elastic medium. In the present model, the longitudinal displacement  $w$  is essentially vanished because of the property of the assumed wave motion. Thus,  $u$  and  $v$  are obtained as follows;

$$\begin{aligned} u &= \left\{ M \frac{\partial H_1^{(1)}(p^*r)}{\partial r} - N \frac{H_1^{(1)}(q^*r)}{r} \right\} \cdot \cos\theta \cdot \exp \{ik^B (x - c^B t)\} \\ v &= \left\{ -M \frac{H_1^{(1)}(p^*r)}{r} + N \frac{\partial H_1^{(1)}(q^*r)}{\partial r} \right\} \cdot \sin\theta \cdot \exp \{ik^B (x - c^B t)\} \end{aligned} \quad (2.22)$$

where  $H_n^{(1)}(z)$  is the Hankel function and  $M$  and  $N$  are constants to be determined from boundary conditions. And the arguments of the Hankel function are given by

$$(p^*)^2 = (\omega/v_l)^2 - (v_l/v_t)^2 (k^B)^2, \quad (q^*)^2 = (\omega/v_t)^2 - (k^B)^2 \quad (2.23)$$

Stress components in the ground are calculated from Eq. (2.23) as follows;

$$\begin{aligned} \sigma_r &= \left[ M \left\{ -\lambda (p^*)^2 \cdot H_1^{(1)}(p^*r) + 2\mu \frac{\partial^2 H_1^{(1)}(p^*r)}{\partial r^2} \right\} + N \left\{ 2\mu \left( \frac{H_1^{(1)}(q^*r)}{r^2} \right. \right. \right. \\ &\quad \left. \left. \left. - \frac{H_1^{(1)}(q^*r)}{r} \right) \right\} \right] \cdot \cos\theta \cdot \exp \{ik^B (x - c^B t)\} \end{aligned} \quad (2.24)$$

$$\begin{aligned} \tau_{r\theta} &= \mu \left[ 2M \left\{ \frac{H_1^{(1)}(p^*r)}{r^2} - \frac{1}{r} \frac{\partial H_1^{(1)}(p^*r)}{\partial r} \right\} + N \left\{ \frac{\partial^2 H_1^{(1)}(q^*r)}{\partial r} \right. \right. \\ &\quad \left. \left. + \frac{H_1^{(1)}(q^*r)}{\partial r^2} - \frac{1}{r} \frac{\partial H_1^{(1)}(q^*r)}{\partial r} \right\} \right] \cdot \sin\theta \cdot \exp \{ik^B (x - c^B t)\} \end{aligned} \quad (2.25)$$

In the next place, we deal with the flexural vibration of the structure under the restraint forces which are induced as the result of the interaction between the structure and the ground. Under the assumption of the complete contact between the structure and its surrounding ground, the following boundary conditions are to be satisfied by solutions.

$$u|_{r=a} = U_p^B \cdot \cos\theta, \quad v|_{r=a} = -U_p^B \cdot \sin\theta \quad (2.26)$$

where  $U_p^B = u_d^B \exp\{ik^B(x - c^B t)\}$ , and  $u_d^B$  expresses the deflection of the structure.

On the other hand  $U_p^B$  must obey the following differential equation for the flexural vibration of a uniform bar.

$$EI \frac{\partial^4 U_p^B}{\partial x^4} + \gamma A \frac{\partial^2 U_p^B}{\partial t^2} = -\gamma A \frac{\partial^2 u^B}{\partial t^2} - F_x^B \quad (2.27)$$

where  $A$ ,  $\gamma$  and  $EI$  are the cross sectional area, the volume density and the modulus of flexural rigidity, respectively.  $F_x^B$  is the restraint force from the ground, which is calculated from Eq. (2.25) as follows:

$$\begin{aligned} F_x^B &= \int_0^{2\pi} (\sigma_r \cdot \cos\theta - \tau_{r\theta} \sin\theta)_{r=a} \cdot a \cdot d\theta \\ &= \rho\pi a^2 \cdot \omega^2 \cdot f^B \cdot u_d^B \cdot \exp\{ik^B(x - c^B t)\} \end{aligned} \quad (2.28)$$

where

$$\left. \begin{aligned} f^B &= \frac{F(p^*a) + F(q^*a) - 4}{F(p^*a) \cdot F(q^*a) - F(p^*a) - F(q^*a)} \\ F(z) &= zH_0^{(1)}(z)/H_1^{(1)}(z) \end{aligned} \right\} \quad (2.29)$$

Substituting Eqs. (2.22) and (2.28) into Eq. (2.27), the amplitude of displacement of the structure for the flexural vibration can be determined as follows;

$$U_p^B = \left\{ 1 + \frac{1}{\frac{EI(k^B)^4}{\gamma\pi(a^2 - b^2)\omega^2} - 1 + \frac{\rho}{\gamma} \frac{1}{1 - (b/a)^2} \cdot f^B} \right\} \cdot u_d^B \cdot \exp\{ik^B(x - c^B t)\} \quad (2.30)$$

On the other hand, the normalized bending strain of the structure is defined by

$$\varepsilon_B^* \equiv a \frac{\partial^2 U_p^B}{\partial x^2} / \frac{u_d^B}{a} = 4\pi^2 \left( \frac{a}{\kappa^B} \right)^2 \frac{U_p^B}{u_d^B} \quad (2.31)$$

where  $\kappa^B$  is the wave length of the incident *SH* wave. Each term of the denominator in Eq. (2.30) is rewritten by the following expressions with non-dimensional variables.

$$\frac{EI(k^B)^4}{\gamma\pi(a^2 - b^2)\omega^2} = \left( \pi \cdot \frac{a}{\kappa^B} \cdot \frac{c^0}{c^B} \right)^2 \left\{ 1 + \left( \frac{b}{a} \right)^2 \right\}, \quad f^B = f^B(p^*a, q^*a) \quad (2.32)$$

$$p^*a = 2\pi \frac{a}{\kappa^B} \sqrt{\left( \frac{c^B}{v_l} \right)^2 - 1}, \quad q^*a = 2\pi \frac{a}{\kappa^B} \sqrt{\left( \frac{c^B}{v_t} \right)^2 - 1}$$

For the same value of  $c^0/\nu_l$ ,  $b/a$ ,  $\nu$ ,  $\kappa^B/a$  with those in case of the longitudinal vibration and for  $c^B/\nu_l=1.5$ , the following results are obtained

$$\left| \frac{EI (k^B)^4}{\gamma \pi (a^2 - b^2) \omega^2} - 1 \right| \approx 0.64, \quad \left| \frac{\rho}{\gamma} \frac{f^B}{1 - (b/a)^2} \right| \approx 456.0 \quad (2.33)$$

Since  $\kappa^B/a$  takes the value greater than 100 considering the wave length of actual seismic waves, therefore, the next inequality would be generally valid.

$$\left| \frac{EI (k^B)^4}{\gamma \pi (a^2 - b^2) \omega^2} - 1 \right| \ll \left| \frac{\rho}{\gamma} \frac{1}{1 - (b/a)^2} \cdot f^B \right| \quad (2.34)$$

The left hand side term of above inequality relates to the vibration characteristics of the structure and the right hand side term shows the effect of the restraint force which is exerting on the structural surface. This implies that the inertia force of the structure is so small compared with the reaction from the surrounding ground that the deflection of the structure is restrained to the extent of that of the ground. Therefore from the results obtained herein it follows that the vibration of the structure itself is hardly evoked by virtue of the existence of the restraining force.

Considering the magnitude of the second term of Eq. (2.30), it is close to zero when the value of  $a/K^B$  is less than 0.01. Thus it may be possible to establish the following approximation in case of  $a/\kappa^B=0.01$ .

$$U_p^B \approx u_g^B \cdot \exp \{ik^B(x - c^B t)\} \quad (2.35)$$

Then the bending strains calculated by Eq. (2.31) is deduced to

$$\varepsilon_B^* \equiv a \frac{\partial^2 U_p^B}{\partial x^2} / \frac{u_g^B}{a} \approx 4\pi^2 \left( \frac{a}{\kappa^B} \right)^2 \cdot \frac{U_p^B}{u_g^B} \quad (2.36)$$

As  $\varepsilon_B$  is defined by  $a \cdot \partial^2 U_p^B / \partial x^2$ , it finally yields

$$\varepsilon_B \approx \left( \frac{2\pi}{\kappa^B} \right)^2 \cdot u_g \quad (2.37)$$

As the term  $(2\pi/\kappa^B)^2 \cdot u_g^B$  is identical with acceleration of the surrounding ground, it is found that the bending strain is closely related to the acceleration amplitude of the ground.

The most important result obtained in this section is that the bending strain induced in the underground tubular structure during earthquakes is almost proportional to an acceleration amplitude of the surrounding ground, while the axial strain is relative to the velocity amplitude.

### 3. Strain Amplitude to Random Excitation

So far the sinusoidal motion of ground has been considered in the analyses described above. In this section the strain amplitude of the structure subjected to a random seismic motion is discussed.  $\varepsilon_A^*$  and  $\varepsilon_B^*$  given by Eqs. (2.14) and (2.31), which are the response to an input of sinusoidal seismic wave can be written as



follows;

$$\left. \begin{aligned} \varepsilon_A/(u_0^A \omega^2) &= \varepsilon'_A(\omega) \cdot \exp\{i\varphi_A(\omega)\} \\ \varepsilon_B/(u_0^B \omega^2) &= \varepsilon'_B(\omega) \cdot \exp\{i\varphi_B(\omega)\} \end{aligned} \right\} \quad (3.1)$$

where  $\omega$  is the circular frequency of incident sinusoidal wave and  $\varepsilon'_A(\omega)$  and  $\varepsilon'_B(\omega)$  denote the frequency response function of strain amplitude and  $\varphi_A(\omega)$  and  $\varphi_B(\omega)$  the phase response. On the other hand, since  $u_0^A \omega^2$  and  $u_0^B \omega^2$  are the acceleration amplitude of sinusoidal ground motion, the left hand side terms of Eq. (3.1) give the frequency response of strain induced in the structure which is subjected to unit amplitude of acceleration with frequency  $\omega$ . By making use of the above frequency response functions, strain response in time domain is obtained for the system subjected to an arbitrary time function  $f(t)$  in place of the sinusoidal seismic wave. Applying the finite Fourier transform technique, strain curve  $\varepsilon(t)$  is calculated by the following formula

$$\varepsilon(t) = \frac{1}{2\pi} \int_0^T H(i\omega) \cdot F(i\omega) \cdot e^{i\omega t} \cdot d\omega \quad (3.2)$$

where

$$\left. \begin{aligned} F(i\omega) &= \int_0^T f(t) \cdot e^{-i\omega t} \cdot dt \\ H(i\omega) &= \varepsilon'_A(\omega) \cdot \exp\{i\varphi_A(\omega)\} \text{ or } \varepsilon'_B(\omega) \cdot \exp\{i\varphi_B(\omega)\} \end{aligned} \right\} \quad (3.3)$$

From the analyses performed in the previous section, it is obvious that  $H(i\omega)$  is the frequency response function which represents essentially the stationary response of the system. Therefore any solution calculated from Eq. (3.2) is inevitably a periodic function with a period which coincides to the record length under the analysis.

However the effects of the periodic property of the solution are not so remarkable provided the period is long enough compared with the record length of excitation. By addition of zeros to the head and tail of the input seismic record  $f(t)$ , the errors caused by the periodic nature of the solution could be avoided. In the numerical computation the F.F.T. algorithm is employed because it effectively reduces the computation time for this kind of calculation, which deals with a great number of date points.

#### 4. Estimate of Strain Amplitude from Accelerograms

Replacing the wave length in Eqs. (2.14) and (2.31) with wave velocity in the ground, we have the following results.

$$\varepsilon_A = \frac{V}{c^A} \cdot \frac{U_p^A}{u_0^A}, \quad \varepsilon_B = \frac{aA}{(c^B)^2} \cdot \frac{U_p^B}{u_g^B} \quad (4.1)$$

where  $V = u_0^A \omega$  and  $A = u_0^B \omega^2$  are the velocity and acceleration of the incident seismic wave, respectively. As is mentioned in Section 2,  $u_0^A$  and  $u_0^B$  are the amplitudes of

displacement and  $c^A$  and  $c^B$  are the phase velocity of longitudinal and transversal waves. As is discussed in the previous section the dynamic behaviour of the underground tubular structures are close to that of the surrounding ground and, therefore, the following expressions may hold good.

$$\frac{U_p^A}{u_0^A} \doteq 1.0, \quad \frac{U_p^B}{u_0^B} \doteq 1.0 \quad (4.2)$$

Under this assumption, the following identities are established.

$$\varepsilon_A \doteq \frac{V}{c^A}, \quad \varepsilon_B \doteq \frac{aA}{(c^B)^2} \quad (4.3)$$

Henceforth, when the maximum values of  $V$  and  $A$  during earthquakes are given, we could readily estimate the maximum strain of the underground tubular structure from the above formulae. Strain amplitude computed from Eq. (4.3) are most likely greater than that computed from Eq. (3.2), which is the result of the analyses that treated the system as a soil-structure interaction system. The difference between strain amplitudes computed from Eq. (3.2) and that from Eq. (4.3) is considered to be the effect of the rigidity of the structure, which is neglected in the latter. The matter is such that the incident energy is appeared to be diminished by the rigidity of the structure. So the ratio of the difference above mentioned to the intensity of incident wave is referred to the loss factor of the incident seismic motion.

In order to compute  $\varepsilon_A$  and  $\varepsilon_B$  from Eq. (4.3) the amplitude of  $V$  and  $A$  are necessary and a method for rough estimate of those values from strong motion accelerograms are discussed. Integrating an acceleration record by numerical method without any correction on the base lines, the resultant velocity or displacement will diverge to have no actual meaning. This is due to various reasons such as the ambiguity of initial velocity amplitude, drift of base line, frequency characteristics of recording instruments and so on. In order to eliminate the divergence of resultant displacement, a filtering of low frequency component is effective so that, in the present paper, a high pass filtering<sup>7)</sup> is applied to the record utilizing the F.F.T. algorithm. Moreover a parabolic-type base line correction method<sup>8)</sup> is applied to all records treated herein.

## 5. Numerical Computation

Numerical computation has been performed to demonstrate the results obtained in the previous sections. Fig. 2 illustrates the relationship between  $\kappa/a$  and  $|f^A|$  and  $|f^B|$  which express the restraining force from the ground. In Fig. 2 is shown the plots of  $|f^A|$  and  $|f^B|$  against the non-dimensional wave length for both of the axial and flexural vibration. In this figure the parameter  $b/a$  expresses the ratio of the inner radius to the outer one. In the computation the following values are used:  $c_0/v_l=10.0$ ,  $\nu=0.40$ ,  $e/\gamma=0.8$ ,  $c^A/v_l=1.5$  and  $c^B/v_l=1.5$ . According to Fig. 2, the restraining force  $|f^A|$  for the axial vibration is smaller than that for the flexural vibration throughout the range of  $\kappa/a$  and this tendency is magnified for longer wave length or smaller

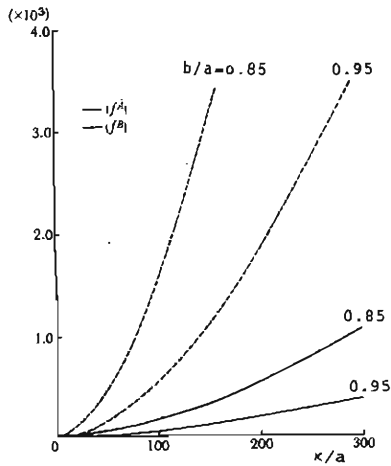


Fig. 2 Relations between restraint forces and  $\kappa/a$

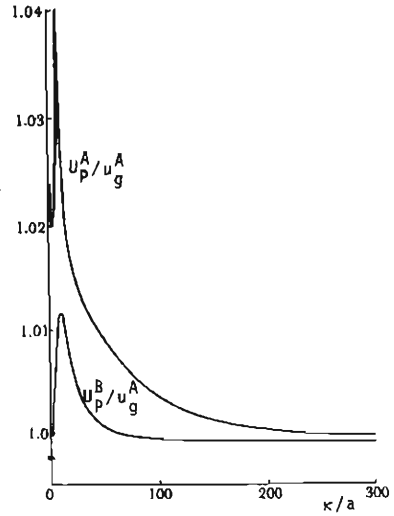


Fig. 3 Frequency response function

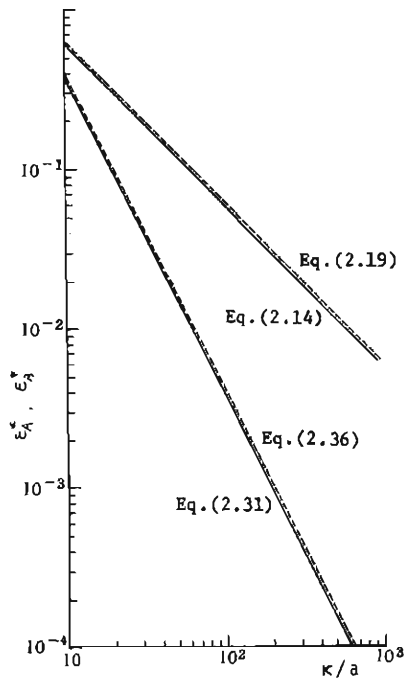


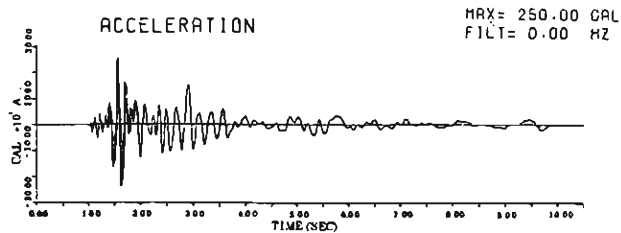
Fig. 4 Relations between strains and  $\kappa/a$

structures. Moreover it is interesting to note that the resisting forces take large values for smaller values of  $b/a$ . This result implies that the resisting force for deformation

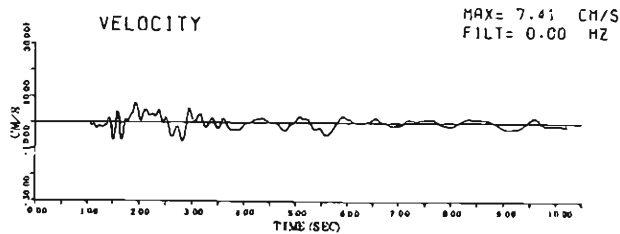
becomes greater as the wall thickness of the structure increases, which is consistent with the results of the theoretical analyses for tunnels performed previously.

Fig. 3 shows the absolute value of the axial and transversal displacement calculated from Eqs. (2.13) and (2.30). Both of the response curves have a single peak at the small range of  $\kappa/a$  and the value of  $\kappa/a$  corresponding to these peaks are considered to be the natural frequency of the structure. These peaks do not appear for large value of the ratio of the wave length to the structural radius and the magnitude of the ordinate tends to unity for both curves. This result implies that the structural response is very close to the ground motion independent of the kind of motion, since the value of  $\kappa/a$  is usually larger than 100.

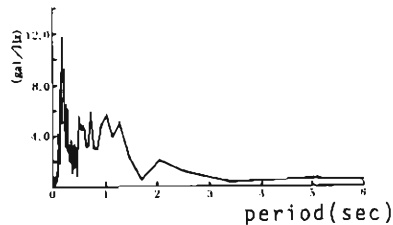
In Fig. 4, the relationship of the axial strain  $\epsilon^*_A$  and bending strain  $\epsilon^*_B$  against  $\kappa/a$  is plotted, in which a logarithmic scale is adopted for both coordinates. It is clearly noticed from Fig. 4 that both  $\epsilon^*_A$  and  $\epsilon^*_B$  are proportional to a certain power of  $\kappa/a$ .



(a)



(b)



(c)

Fig. 5 Accelerogram and its Fourier spectrum

As the gradients of these lines are found to be  $-1.0$  for axial strain and  $-2.0$  for bending strain, the axial strain is inversely proportional to the wave length and the bending strain is to the square of the wave length. As the frequency of wave is the reciprocal of wave length, axial strain is proportional to the velocity amplitude of the ground and the bending strain is proportional to the acceleration amplitude. The dotted lines in the same figure are plotted for the computed value from Eqs. (2.19) and (2.36). Although the values of the dotted lines are greater than that of the solid lines, only a slight difference is observed between the corresponding two lines for the full range of  $\kappa/a$ . This difference is considered to be the loss factor caused by the rigidity of the structure.

In the next, the numerical computations of strain curve to random excitations were performed. Fig. 5(a) illustrates an accelerogram used as an incident wave in the numerical computation, which was recorded on a ground surface at Wakayama city during the earthquake which occurred on March 30, 1968 and the velocity curve integrated from the accelerogram is shown in Fig. 5(b). The Fourier spectrum is shown in Fig. 5(c) and the predominant period is read to be 0.19 sec from this spectrum. By the method described in Section 3, the axial and bending strains were computed for the case of  $v_i=100$  m/sec,  $a=2$  m and the other non-dimensional constants were kept same with those values which were used in the case shown in Fig. 4. The frequency response functions versus strain amplitude are shown in Fig. 6 for the case under consideration. Examples of the time history of the axial and bending strain are shown in Fig. 7. In the computation, in order to eliminate the periodicity in the solution, records with zero amplitude of 1.88 sec duration were attached to the head and tail of every original accelerogram. Comparing Figs. 5(b) and 5(a) with Figs. 7(a) and 7(b) respectively, it is found that the time history for the bending strain is quite similar to the accelerogram. Moreover it should be noted that the time history of axial strain is close to the velocity curve which was obtained by the integration of the accelerogram.

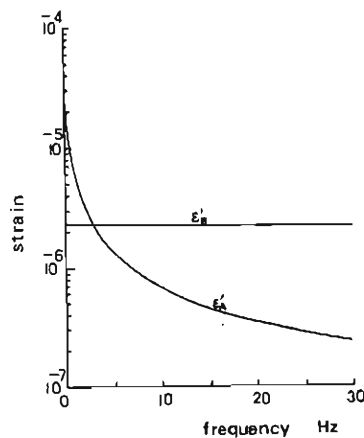


Fig. 6 Frequency response functions of strains

Figs. 8(a) and 8(b) show the Fourier spectra of the axial and bending strain, respectively. Comparing two spectra shown in Figs. 5(c) and 8(b), it is obvious that the bending strain has close relations with the acceleration of the ground. In Fig. 9 plotted is the relationship between S-wave velocity of the ground and the maximum strains induced in the structure to the incidence of accelerogram shown in Fig. 5(a).

The plots of the maximum strains against the radius of structure are shown in Fig. 10 which indicates that the bending strain is proportional to the radius of struc-

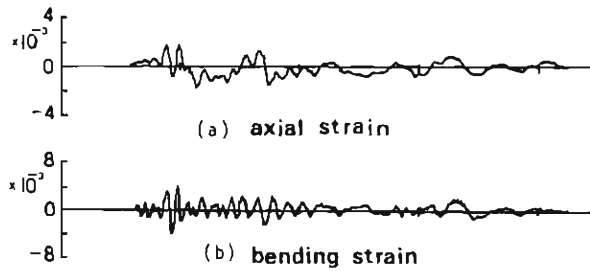


Fig. 7 Strain curves

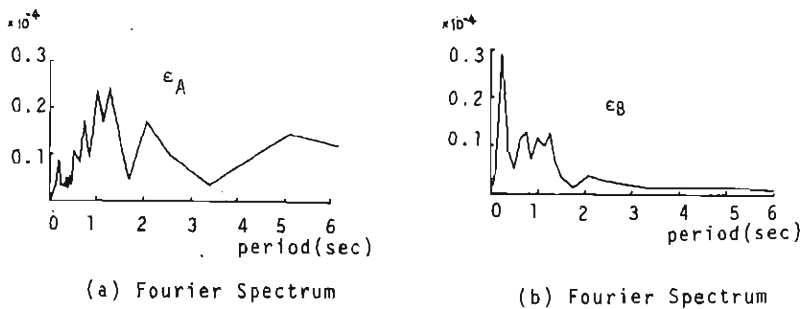


Fig. 8 Fourier spectra of strains

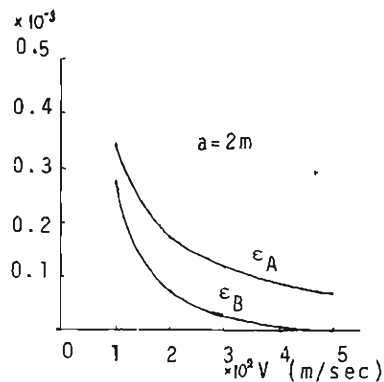


Fig. 9 Relations between strains and S-wave velocity

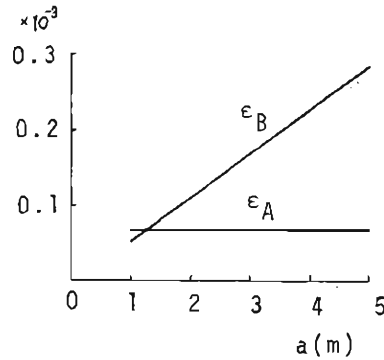


Fig. 10 Relations between maximum strains and structural radius

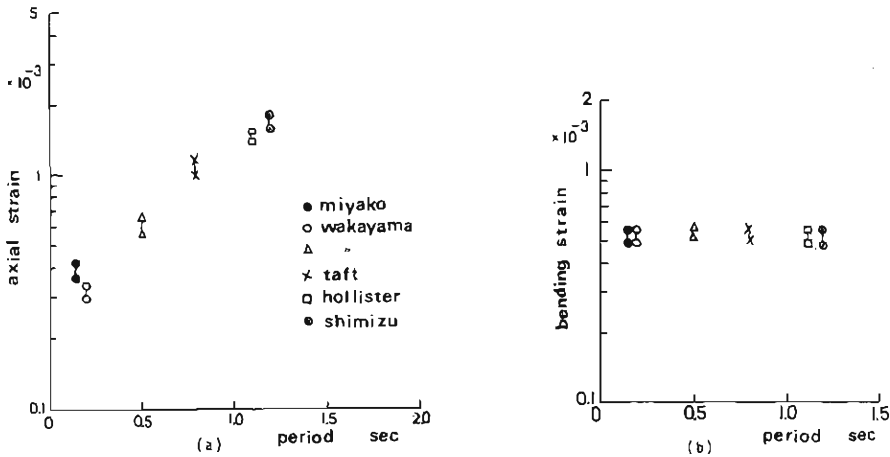


Fig. 11 Relations between maximum strain and predominant period of accelerograms

ture while the maximum axial strain is independent of the radius of structure. Therefore this figure implies a notable fact that the bending strain is dominated and significant in a structure with large sectional area such as subway tunnels and that in contrast, the axial strain is important for underground pipe systems.

Effects of the predominant period of earthquakes to the maximum strain are illustrated in Figs. 11(a) and 11(b). Six accelerograms listed in Table 1 were used as incident seismic waves. Records were modified so that the maximum acceleration is 250 gals. While the axial strain is proportional to the predominant period of the incident earthquake records, the bending strain is almost independent of the period. In these figures, the upper plots for each of the six records were calculated from the approximate method given by Eq. (4.3) and the lower plots were from Eq. (3.2), which was derived from the analyses taking the interaction between the structure and ground into consideration. But, the difference between corresponding two plots computed from the different methods is not so remarkable and values computed from

Eq. (3.2) are smaller than the values computed from Eq. (4.3) by 10–20%. This difference is evidently due to the stiffness of structures as discussed previously. It is notable that the amount of the difference is almost the same for any records as long as the accelerograms analysed in the present paper are concerned. This is again consistent with the results shown in Fig. 4 as the wave length used in abscissa of Fig. 4 is readily transformed to the period.

In Fig. 12 shown is the plots of the maximum velocity amplitude obtained by numerical integration of accelerograms against the corresponding maximum acceleration amplitude. In addition to the accelerograms listed in Table 1, another 55

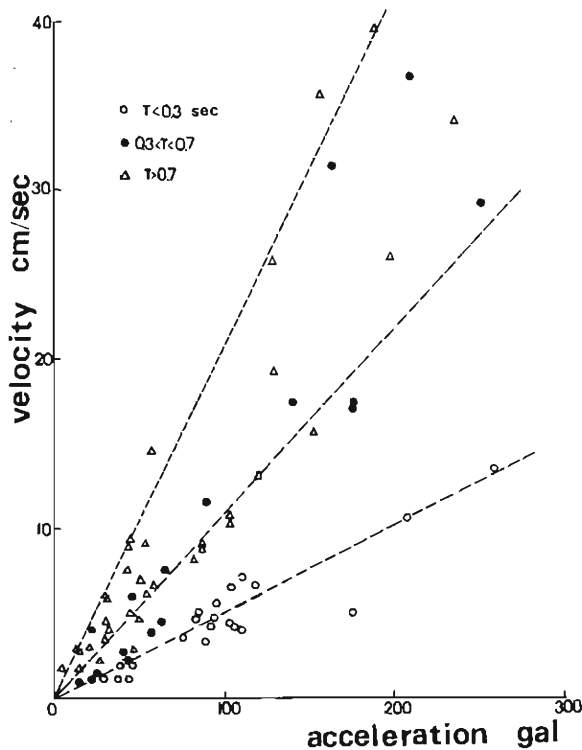


Fig. 12 Relations between maximum velocity  $V_m$  and maximum acceleration  $A_m$

Table 1 Data for earthquake record treated

Data No.	Location	Date	Max. Acc. (gal)	Predominant Period (sec)
S074N	Shimizu	1965.4.20	86.3	1.28
S236N	Miyako	1968.5.16	118.0	0.18
S265N	Wakayama	1968.3.30	176.0	0.19
S265E	Wakayama	1968.3.30	258.0	0.51
IIA04N	Taft	1952.7.21	153.7	0.73
IIA18E	Hollister	1961.4.4	175.7	1.10



accelerograms were analysed to obtain these plots. These accelerograms were classified into three groups depending on their predominant period  $T$  as shown in the figure. Denoting the maximum acceleration amplitude by  $A_m$  and the maximum velocity amplitude by  $V_m$ , the following approximate representations are possibly adopted for each group.

$$\begin{aligned}
 T > 0.7 & \quad V_m \doteq 0.2 A_m \\
 0.3 < T < 0.7 & \quad V_m \doteq 0.1 A_m \\
 T < 0.3 & \quad V_m \doteq 0.05 A_m
 \end{aligned}
 \tag{5.1}$$

( $A_m$  : gal,  $V_m$  : kine)

A more important result is obtained which concerns the relationship of the maximum velocity amplitude to the predominant period of the corresponding accelerograms, which is shown in Fig. 13. In advance of the computation, all records were scaled to have the same maximum amplitude of 250 gals. Applying the least squares method to these plots, the following expression is obtained.

$$V_m \doteq 16.5 T^{0.58} \quad (\text{for } A_m = 250 \text{ gal})
 \tag{5.2}$$

These empirical formulae enable us to estimate the maximum velocity amplitude when the maximum acceleration for the design purpose is given. Once the maximum acceleration and velocity amplitudes are determined, a rough estimate of the upper

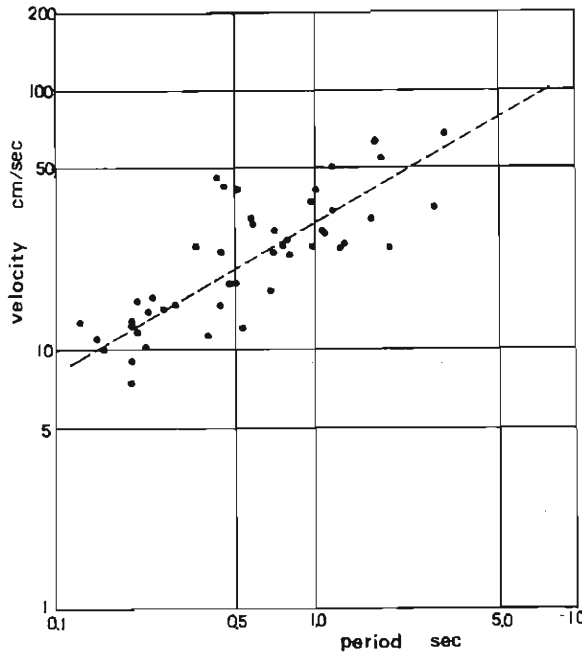


Fig. 13 Relations between maximum velocity  $V_m$  and predominant period  $T$

bound of the strains induced in the underground tubular structures are readily calculated from Eq. (4.3). Moreover, in order to estimate the actual strains in structure, these strains are to be reduced by the lossfactor from 0.1 to 0.2.

## 6. Conclusion

The main conclusions derived from this study are summarized as follows:

1) As far as the underground tubular structure with uniform physical property is concerned, the structural vibration caused by its inertia force is hardly excited in ground. This is attributed to the fact that the inertia force of this kind of structures is usually negligibly small compared with the restraining force which the surrounding ground exerts on the structural surface.

2) Reaction force per unit length of structure is remarkable in the flexural motion of the structures rather than the axial motion and it is proportional to the squares of the ratio of the wave length to the structural radius.

3) Axial strain induced in the underground tubular structures during an earthquake is greater than the bending strain for the large value of the ratio of the wave length to the structural radius. When, however, the radius of the structure exceeds a few meters, the bending strain dominates in the structure instead of the axial strain.

4) The bending strain increases in accordance with the acceleration amplitude in ground while the axial strain is proportional to the velocity amplitude. These results suggest that, excepting for the wave with an extremely short period, the velocity amplitude in ground is the most significant factor in the aseismic design of the underground tubular structure with small diameter, while the acceleration amplitude is of importance for the structures with large diameter such as subway tunnels.

5) Strain levels induced in the structure are reduced by 10 to 20% of strain in the surrounding ground as the result of interaction between the structure and ground. Then the strain in ground is considered to be the upper bound of the strain in structures.

6) From the results of numerical computation of the strain curve to several strong motion accelerograms, it can be said that the maximum bending strain in structure with radius of 2 m is estimated to be the order of  $0.6 \cdot 10^{-3}$  when the ground, in which S-wave velocity is assumed to be 100 m/sec, is subjected to the acceleration with maximum amplitude of 250 gals. However, the axial strain reaches to the extent of  $1.0 \cdot 10^{-3}$  for the incident wave with predominant period of 1.0 sec and this value can increase for an increasing predominant period.

## References

- 1) Kuessel, T.R.: Earthquake Design Criteria for Subways, Proc. ASCE, No. ST6, 1969, pp. 1213-1231.
- 2) Goto, H., K. Toki and S. Takada: Vibrational Characteristics of Underground Pipe, Annuals of Disaster Prevention Research Institute, Kyoto Univ., No. 15B, 1972, pp. 513-

526.

- 3) Okamoto, S., C. Tamura, K. Kato and M. Hamada: Behaviors of Submerged Tunnels during Earthquakes, Proc. 5WCEE, Rome, 1973.
- 4) Sakurai, A., T. Takahashi, C. Kurihara and H. Yajima: A Proposal for Earthquake Response Analyses of Long Structures, Proc. JSCE, No. 186, 1971, pp. 25-38.
- 5) Aoki, Y.: Seismic Design Spectra for Trench Type Tunnel, Proc. JSCE, No. 211, 1973, pp. 77-87.
- 6) Goto, Y., J. Ota and T. Sato: On the Earthquake Response of Submerged Tunnels, Proc. 5WCEE, Rome, 1973.
- 7) Hudson, D.E.: Some problems in the Application of Spectrum Technique to Strong Motion Earthquake Analysis, Bulletin of the Seismological Society of America, Vol. 52, No. 2, 1962, pp. 417-430.
- 8) Trifunac, M.D.: Strong-Motion Earthquake Accelerograms Digitized and plotted Data, Vol. II, Part A, Earthquake Engineering Research Laboratory, EERL 71-50, California Institute of Technology, Pasadena, Sept., 1971, pp. 3-22.